Iranian Journal of Chemical Engineering
Vol. 7, No. 3 (Summer), 2010, IAChE

Simulation and Experimental Investigation of the Permeability Reduction due to Asphaltene Deposition in Porous Media

S. Ashoori[1], A. Khaksar Manshad[2], N. Alizadeh[3], M. Masoomi[4], S. H. Tabatabaei[4]*

1-Department of Petroleum Engineering, Petroleum University of Technology, Ahwaz, Iran
2- Department of Chemical Engineering, School of Engineering, Persian Gulf University, Boushehr 75168, Iran
3-Department of Petroleum Engineering, University of Amir Kabir, Tehran, Iran
4- Department of Petroleum Engineering, Omidieh Islamic Azad University, Ahwaz, Iran

Abstract

A static to dynamic approach to modeling Asphaltenes has been developed and validated. A new algorithm for static asphaltene modeling uses a multi-solid thermodynamics approach where the equality of fugacity for each component and phase is applied at equilibrium conditions. This is required for minimizing the Gibbs free energy. The fractal distribution function used for the splitting and characterization of heavy components provides accurate results. The precipitation and re-dissolution of asphaltenes are investigated for a relatively heavy crude oil from an Iranian field. A series of experiments are designed and carried out quantitatively to obtain the permeability reduction in a slim tube. Using a dynamic reservoir simulator, a 3-dimensional asphaltene model is developed to simulate the precipitation, flocculation, deposition and its impact on permeability in a slim tube. With this approach, the asphaltene is defined as a set of component(s) that can precipitate depending on their molar percentage weight in the solution. The simulated permeability reduction due to asphaltene deposition shows good agreement with our experimental data

Keywords: *Permeability Reduction, Slim Tube, Asphaltene Precipitation*

1- Introduction

Asphaltenes can reduce hydrocarbon effective mobility by:

a) Blocking pore throats thus reducing rock permeability.
b) Adsorbing onto the rock and altering the formation wettability from water-wet to oil-wet, hence diminishing the effective permeability to oil and increasing the irreducible oil saturation.
c) Increasing the reservoir fluid viscosity by forming a colloidal solution in the oil phase.

The permeability reduction due to asphaltene particles deposition in porous media is the most dominant damage mechanism in the cases of asphaltene-induced formation damage in the reservoirs where under

∗ Corresponding author: khaksar58@yahoo.com

saturated oil is being produced without water. The damage radius depends on draw down and usually occurs many feet inside the reservoir. Several authors have studied different models for asphaltene deposition in core tests. Civan et al. [1, 2] assume that the flow channels in porous media are grouped into plugging and non-plugging pathways, and for the deposition model they use surface adsorption, pore throat plugging, and entrainment of deposits. Ali and Islam [3] assume that Asphaltene is suspended in crude oil and ready to deposit, and for the deposition model the surface adsorption and entrainment of the deposits are considered. Wang et al. [4] assume Asphaltene precipitation can be simulated by ideal solution theory, and for the deposition model surface adsorption, plugging, and entrainment as in [5] are used.

2- Slim tube experiments

2.1- Materials and apparatus

The crude oil under investigation is a relatively heavy oil with a gravity index of 20°API sampled from an oil field in southwestern Iran, (see Table (1)). The asphaltene content of the oil is 11% by weight. The crude oil is stored under laboratory conditions for up to three months to allow any volatile component to evaporate, in order to establish equilibrium and obtain a crude oil with a relatively fixed composition. The oil is then filtered by standard filter paper (Wattman No. 42) to ensure minimal sand or clay content usually associated with produced oils.

In all experiments, pure n-heptane is used as the precipitant, and the gravimetric method is used for measuring the amount of asphaltene precipitated.

Table 1. Composition and characteristics of the crude oil

Component	**Oil Sample**
H_2S	0.192
Nitrogen	0
CO_2	2.204
Methane	26.945
Ethane	8.008
Propane	6.426
i-Butane	1.134
n-Butane	3.682
i-Pentane	1.742
n-Pentane	2.233
Hexanes	4.202
Heptanes+	43.212
RESERVOIR OIL M.W. (gr/grmole)	156.67
Test Temperature (F)	225
MW C7+ (gr/grmole)	316.49
SG C7+	0.9272
density of reservoir fluid @ Pb (gr/cc)	0.7646
Bubble point pressure (psia)	1890
Asphaltene content in stock tank oil, wt%	11

To understand the phenomenon of asphaltene deposition at reservoir conditions, several experiments were conducted with a synthetic porous medium at high pressure and high temperature.

The experimental setup is illustrated in Fig. 1. It contains a slim tube, oil bath, vacuum pump, liquid pump, fluid transfer vessels, a capillary sight glass with a heating jacket for visual observation of passing fluid, a back pressure regulator for the produced oil, a flask for collecting the produced oil, pressure gauges, pipes, valves and fittings.

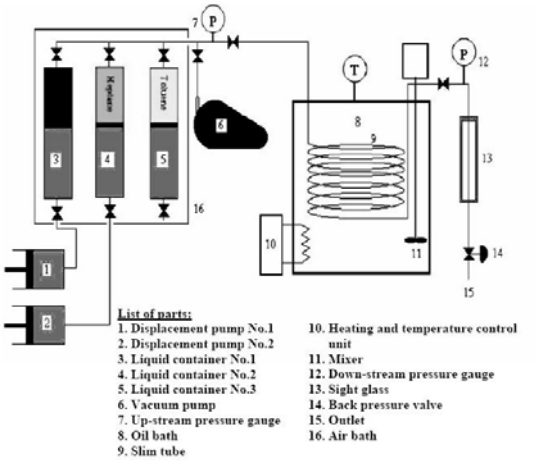

Figure 1. A schematic diagram of the experimental setup

To determine the amount of permeability reduction by asphaltene precipitation and deposition in porous media, a Ruska slim tube is used. The slim tube is a narrow stainless steel tube coil of 7.9 mm O.D. and 6.2mm I.D. The tube length is 18.3 m (60 ft), coiled to a diameter of roughly 20 cm. The tube is packed with 150 to 170 micron round grained glass beads.

The porous media has an overall porosity of approximately 27% and an absolute permeability of approximately 5 darcies (4.93×10^{-12} m^2). The total system pore volume, including lines and fittings, is approximately 150 cm^3. The slim tube (the one dimensional reservoir model) is located in an oil bath.

The constant temperature oil bath is a thermostatically controlled heat insulated tank capable of reaching 175°C, and has a volume of approximately 0.06 m^3 (60 liters). A duct contains the heating elements and circulating stirrer. This arrangement assures complete circulation of the fluid through the bath and keeps the equipment space in the bath free from any obstruction. The bath is equipped with an adjustable temperature controller with a resolution of 1°C. The slim tube is situated vertically in the bath, while both its inlet and outlet valves are mounted on the top of the bath. The bath operates with the oil level above the slim tube to ensure uniform temperature distribution along the slim tube. Located on the downstream end of the slim tube is a high-pressure capillary sight glass with a heating jacket, which allows observation of the produced fluids. These observations identify the passage of a single phase or gas and liquid slug flow.

Upstream pressure is monitored with a pressure gauge, and another is connected downstream of the slim tube. The operating pressure envelope is controlled by a downstream back pressure regulator after which the produced oil is flashed to atmospheric conditions.

The pump consists of two individual cylinder-piston arrangements with a volume of 500 cm^3 per cylinder. The pump flow rate is variable from 1 cm^3/hr to 1999 cm^3/hr. A calibrated ruler is installed between the two cylinders, enabling reading of the outlet volume with an accuracy of 0.0025 cm^3. The pump is a motor-operated, computer-controlled positive displacement pump with a 70,000 kPa maximum working pressure equipped with mechanisms permitting manual operation as well.

3- Experimental activities

The experimental procedures can be divided into two major categories:

3.1- Preliminary activities

The preliminary activities consisted of:

a. Washing the slim tube
b. Drying the slim tube
c. Evacuating the slim tube
d. Filling the fluid transfer vessels
e. Pore volume measurement
f. Investigating the flow behavior of the system
g. Permeability measurement
h. Calculation of packed bed porosity by Carman-Kozeny equation

3.2- Flooding experiments

A series of flooding experiments were carried out to determine the effect of solvent to oil ratio, injection rate and temperature as the permeability reduces over time in the porous medium due to asphaltene deposition. n-heptane was used as a solvent in this work. The rate of injection into the porous medium was determined such that the Reynolds number was less than or equal to unity in order to apply Darcy's law for determining the permeability.

The preliminary work discussed previously is necessary for providing the operating conditions for the porous medium flood tests. The procedure of the flood test is as follows:

1. One of the piston-equipped fluid transfer vessels is filled with filtered crude oil, and another with n-heptane.
2. The vessels are connected to each other by means of two lines connected to the top valve of each vessel, with a T-junction in-between.
3. A pump is connected to the bottom valve of each vessel, then each pump is adjusted to the desired flow rate and the system evacuated from trapped air.
4. The outlet of the T-junction is connected to the inlet of the porous medium, which was previously evacuated, while the inlet valve is closed.
5. Injection of both fluids is started and the crude oil and n-heptane are allowed to mix. The inlet valve to the porous medium is opened simultaneously with the pump being activated. The starting time of the injection is recorded.
6. The inlet pressure of the porous medium is recorded every 2 minutes. The mixture of the crude oil and n-heptane flows through the porous medium. After injecting about one pore volume (150 cm^3) of the mixture into the porous medium the inlet pressure begins to rise. The outlet valve is then opened and the mixture produced. The inlet pressure begins to drop and reaches steady state condition within a short time. The pressure then increases continuously due to asphaltene deposition in the porous medium. When the mixture is observed at the outlet of the porous medium, a sample with a volume of about 10 cm^3 is collected every 10 minutes. The sampling operation is continued until a minimum of 4 pore volumes of fluid have been injected into the slim tube. If the pressure exceeds 28,000 kPa, the experiment is terminated for safety considerations.
7. The samples collected from step 6 are used to determine the asphaltene precipitated, leaving the slim tube the and remainder in these samples.

Based on data obtained in part 6, and

applying Darcy's law, the permeability of the porous medium versus time, or the pore volume of the fluid injected can be calculated for different experiments. By performing such experiments and analyzing the experimental results one can determine the effects of different parameters on the severity of permeability impairment due to asphaltene deposition in the porous medium. Data obtained in step 7 provide the concentration of precipitated asphaltene in the effluent versus time for each experiment. The conditions of these experiments (input parameters) are given in Table 2.

4- Thermodynamics model formulation

Consider a system of N_s precipitating species and N components. The equations for phase equilibrium are:

(1) N vapor-liquid iso-isofugacity equations:

$$f_i^v(P,T,y_1,y_2,....,y_{N-1}) - f_i^l(P,T,x_1,x_2,....,x_{N-1}) = 0 \quad \text{(i=1, N)} \tag{1}$$

(2) N_s liquid-solid iso-isofugacity equations:

$$f_i^l(P,T,x_1,x_2,....,x_{N-1}) - f_{pure,i}^s(P,T) = 0$$

$$[\text{i= (N- } N_s\text{) +1, N}] \tag{2}$$

(3) N-1 material-balance equations:

(a) For the non precipitating components:

$$z_i - x_i^l\left[1 - \sum_j^{N_s} S_j / F - \frac{V}{F}\right] - K_i^{vl} x_i^l \frac{V}{F} f_i^l = 0$$

$$[\text{i= 1, (N- } N_s\text{)}] \tag{3}$$

Table 2. input parameters (test conditions).

Parameters	Test #1	Test #2	Test #3	Test #4	Test #5	Test #6
Flow rate, (cm3/hr)	60	30	30	60	90	30
Concentration of n-C7 In the mixture, (%)	40	40	60	50	40	50
Concentration of asphaltene in the mixture, (vol./vol.)	0.001811	0.001811	0.003066	0.002462	0.001811	0.002462
Mixture density, (g/cm3)	0.808	0.808	0.77	0.79	0.808	0.79
Asphaltene density, (g/cm3)	1.1	1.1	1.1	1.1	1.1	1.1
Mixture viscosity, (CP)	1.1	1.1	0.59	0.71	1.1	0.71
Total length of porous medium, (cm)	1828.8	1828.8	1828.8	1828.8	1828.8	1828.8
Cross-section area of porous medium, (cm2)	0.30	0.30	0.30	0.30	0.30	0.30
Temperature, (°C)	90	90	90	90	90	90

(b) For precipitating components where all solid phases are pure:

$$z_i - x_i^l\left[1-\sum_j^{N_s} S_j / F - \frac{V}{F}\right] - S_i / F - K_i^{vl} x_i^l \frac{V}{F} f_i^l = 0$$

$$[i=(N-N_s)+1 \ldots N-1](N_s>1) \quad (4)$$

Where K_i^{vl} are the K-values defined by $K_i^{vl} = \frac{\varphi_i^l(T,P,x^l)}{\varphi_i^v(T,P,y)}$.

4.1- Molecular weight distribution calculation

The determination of the molecular weight of asphaltene is a very important step towards the characterization of these substances and thus a great deal of effort has been devoted to this aim. However, due to several factors, such as the poly-dispersivity of the sample, difficulties in isolating asphaltene from crude oil and the tendency of the sample to form aggregates in crude oil and in organic solvents, the asphaltene molecular weight has proven to be very difficult to determine. Thus, it is not surprising that an asphaltene molecular weight value between 1000 and 300000 gr/grmole has been reported for asphaltenes [4].

The molecular weight of asphaltene is usually determined by gas permeation chromatography (GPC) technique, as it gives the average molecular weight and the molecular weight distribution (MWD) value for asphaltene. Table (3) shows the MWD and the average molecular weight of the oil sample, which is used in this study.

Since asphaltene is characterized as a continuous mixture that follows a distribution function, we have examined different types of distribution for selecting the most accurate molecular weight distribution function. Also in this paper, we compare the asphaltene molecular weight distributions obtained from our experiments with theoretical distribution functions. The parameters of each function are adjusted using the asphaltene experimental data [7, 8].

Table 3. Distribution and Average molecular weight of asphaltene for crude oil

	Oil sample
Molecular weight distribution	Molecular weight
10%	331.2
30%	542.98
50%	852.06
70%	1473.4
90%	4934.2
Average molecular weight	1930.2

The most common theoretical distribution functions are: gamma distribution function [7], Schultz-Zimm distribution function [9], fractal distribution function [8], and resin distribution function [7]. Resin distribution function is explained here in detail.

4.2- Resin distribution function

The Resin distribution function is given as [7]:

$$F(Mw_{ai}, c_R) = \frac{(1-w)^{1-w} Mw_{ai}^{-w} \exp[-(1-w)Mw_{ai}]}{\Gamma(1-w)} \quad (5)$$

Where the parameters of the Resin distribution function are obtained as:

$$w = f(c_R) = c_2 + c_2\sqrt{c_R} \quad (6)$$

$$\langle Mw_{ai} \rangle = Mw_{a0}^{\frac{1-f(C_{R0})}{1-f(C_R)}} \quad (7)$$

The adjusted parameters for theoretical MWD are reported in Table (4) and the results are compared in Fig. (2).

4.3- Phase stability test for Solid-Liquid Equilibrium of precipitating components

Each pure component that separates from the initial phase is imported to the solid phase as a pure solid component, hence:

$$\Delta G_{Demixing} = -\Delta G_{mixing} = -\varepsilon(\mu_j^0 - \mu_j) \quad (8)$$

Table 4. parameters for different distribution functions (oil sample)

Distribution functions	C_{R0}	C_R	C_1	C_2	ω	η	Mw_0
Gamma	-	-	-	-	-	270840	257
Schultz	-	-	-	-	-	-	100
Fractal	-	-	-	-	- 0.9307	-	200
Resin	0.5	0.84	- 0.44735	- 0.18545	-	-	200

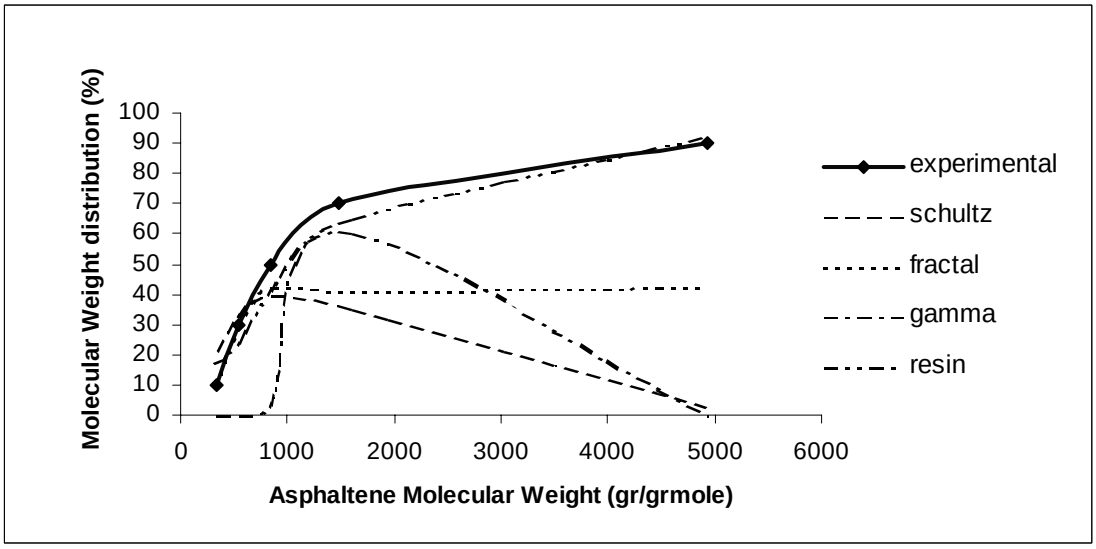

Figure 2. Comparison of several theoretical MWD with experimental MWD for our oil sample

where μ_j^0 is the chemical potential of component j in the first state (μ_j^L) and μ_j is the chemical potential of the component j in the new state ($\mu_{j,pure}^S$). Stability of the original mixture, z_i, requires that for all compositions y_i, the Gibbs free energy G_0 is always less than that for the two-phase split. In other words,

$$\Delta G_{mixing} \leq 0 \tag{9}$$

In addition, for phase instability we have:

$$\Delta G_{mixing} \geq 0 \tag{10}$$

Then, we can say:

$$\Delta G_{mixing} = \mu_j^0 - \mu_j = \mu_j^L - \mu_{j,pure}^S \geq 0 \tag{11}$$

On the other hand, we have:

$$\mu_j^L - \mu_{j,pure}^S = RT \ln(\frac{f_j^L}{f_{j,pure}^S}) \geq 0 \rightarrow (\frac{f_j^L}{f_{j,pure}^S}) \geq 1 \tag{12}$$

Finally, for each multi-solid component formation, we must have:

$$f_j^L(T,P,z_j) - f_{j,pure}^S(T,P) \geq 0 \tag{13}$$

Inequality (13) shows that if the fugacity difference of component j in the liquid phase and the fugacity of this component in the pure solid phase is greater than or equal to zero, then component j will appear in the solid phase.

5- Asphaltene simulation model

Using a dynamic reservoir simulator Ecllipse 300, a 3-dimensional asphaltene model is developed to simulate the precipitation, flocculation, deposition and its impact on permeability in a slim tube.

5.1- Asphaltene characterization and precipitation

Asphaltene is characterized by a set of hydrocarbon component(s) that have the ability to precipitate depending on the reservoir conditions. The variables that can be used to monitor the reservoir conditions are either the pressure (P), the temperature (T), or the molar fraction of a given component (Z), or a combination of two of those variables. The precipitation is then set as the capability of the oil phase to dissolve the asphaltene component(s) as a function of either P, T, Z, or a combination or two of those variables. This provides a simple and flexible way to use laboratory data directly in the simulator. The amount of precipitate corresponds to the excess of a specified component in the oil phase with respect to the limit defined in the model as a function of P, T or Z (or two of those variables).

5.2- Asphaltene flocculation

Once precipitation has started aggregation of the fine precipitate particles can follow. We refer to this coarsening process as flocculation. This process can be reversible, allowing bigger particles, the flocs, to dissociate into fine again.

5.3- Asphaltene deposition

The flocs can then adsorb on the rock surface, can be trapped within the porous media because of their size (plugging) or can be entrained and returned to the oil phase

because of high, local velocity (shear). The deposition in the flow direction *i* is modeled as follows:

$$\frac{\partial \varepsilon_i}{\partial t} = \frac{\alpha}{d}\phi C_a + \gamma |F_{oi}| C_a - \beta \left(|U_{oi}| - U_{cr} \right)^+ \varepsilon_i \tag{14}$$

where *d* is the dimension of the problem (1D, 2D or 3D) and:

- ε_i is the volume fraction of the deposit in the *i* direction of the flow,
- α is the adsorption or static deposition coefficient,
- ϕ is the current porosity (time t),
- C_a is the volumetric concentration of the flocs in the oil phase (flowing flocs),
- F_{oi} is the oil Darcy flux,
- γ is the plugging coefficient,
- β is the entrainment coefficient,
- U_{oi} is the oil phase velocity ($F_{oi}/(A\phi)$, A is the section area between the connecting cells,
- U_{cr} is the critical velocity.

The '+' sign around the bracket for the entrainment part means that the entrainment will be zero if the velocity $|U_{oi}|$ is smaller than the critical value U_{cr}. The overall volume fraction deposit is the sum of the deposits in each direction *i*:

$$\varepsilon = \sum_{i=1}^{d} \varepsilon_i \tag{15}$$

The flocs mole fraction that deposits is taken as:

$$n_a^{dp} = \varepsilon n_a^f \tag{16}$$

And the flocs mole fraction that remains in the solution is corrected to:

$$n_a^f = n_a^f - n_a^{dp} \tag{17}$$

The concentration of the flowing part of the flocs is calculated as:

$$C_a = \frac{n_a^f S_o x_a}{b_o} \tag{18}$$

Where b_o is the oil molar density, S_o is the oil saturation, and x_a the molar fraction of the flocs in the liquid phase. Deposition parameters α, γ, β, and U_{cr} are input parameters obtained from the experimental data.

5.4- Plugging control

The transport equation (14) is slightly altered to take into account some of the plugging aspects more accurately. Here, the plugging can be delayed by specifying a critical volume fraction of asphaltene deposit ε_{cr} and a critical concentration of flocs C_{acr}, above which the plugging can happen:

$$\frac{\partial \varepsilon_i}{\partial t} = \frac{\alpha}{d}\phi C_a + \gamma |F_{oi}| (C_a - C_{acr}) - \beta \left(|U_{oi}| - U_{cr} \right) \varepsilon_i \tag{19}$$

Basically, the coefficient γ is set as:

$$\gamma = \begin{cases} \gamma_0 & \text{if } \varepsilon > \varepsilon_{cr} \text{ and/or } C_a > C_{acr} \\ 0 & \text{otherwise} \end{cases} \tag{20}$$

This means that plugging will occur only if the flocs concentration gets above the critical value and/or the volume fraction deposit

becomes bigger than the critical value. It should be noted that when the concentration gets above critical, only the concentration difference would contribute to the plugging. The critical volume fraction of the asphaltene deposit can be interpreted as a reduction in the average pore radius. Using the empirical correlation and Eq. 23 (below), a critical radius can be estimated as:

$$r \approx \sqrt{\frac{K}{\phi}} \rightarrow r_{cr} \approx r_o \left(1 - \frac{\varepsilon_{cr}}{\phi_o}\right)^{\frac{\delta-1}{2}} \quad (21)$$

So the remaining flow radius is $r = r_0 - r_{cr}$. Exponent δ is the same as in Eq.34 below. The critical flocs concentration can be interpreted, as a likelihood that above that value the size of some of the flowing flocs is big enough to plug some pore throats.

5.5- Asphaltene Damage

Porosity

One type of damage associated with asphaltene deposition is a reduction in porosity due to asphaltene deposition that can be written as:

$$\phi = \phi_0 - \int_0^t \frac{\partial \varepsilon}{\partial t} dt \quad (22)$$

where ϕ_0 is the initial porosity and ε is the volume fraction of the asphaltene deposit.

Permeability

If the rock permeability is correlated to the porosity, a reduction in permeability can also be taken into account using a parameterized power law relationship given the ratio of the permeability K at time t with respect to the initial permeability K_0:

$$\frac{K}{K_o} = \left(1 - \frac{\varepsilon}{\phi_0}\right)^{\delta} \quad (23)$$

The exponent, δ, should be specified based on core experiment data. Alternatively, if the rock permeability is independent of the porosity, or data giving a relationship between the permeability and the amount of asphaltene deposit are available, this can be directly used within a look-up table.

Oil viscosity

When precipitation occurs, asphaltene fines can be considered as colloids in the oil phase, which can alter the viscosity of the transporting phase, i.e. oil phase. The viscosity alteration can be modeled in three different ways:

1- Generalized Einstein model (one parameter):

$$\frac{\mu}{\mu_0} = 1 + aC_p \quad (24)$$

where the default for a is 2.5, and C_p is the volume concentration of the precipitate, and μ_0 is the oil viscosity at C_p=0. The coefficient a should be specified in the model. This model should be used for highly diluted colloids.

2- Krieger and Dogherty model (two parameter):

$$\frac{\mu}{\mu_0} = \left(1 - \frac{C_p}{C_{p0}}\right)^{-\eta C_{p0}} \quad (25)$$

where η is the intrinsic viscosity, η=2.5, for asphaltene colloids. C_{p0} is the volumetric

concentration for maximum packing, equal to 0.65 for spheres packing.

3- Look-up table, giving the oil viscosity multiplier as a function of the volume fraction of the asphaltene precipitate. The first column is the volume fraction and the second column is the viscosity multiplier.

Wettability change

Asphaltene deposition can trigger a wettability change. The exact physics on how this alteration occurs is still a research topic, however, it has been reported that some of its effect can be captured by a relative permeability shift from a water-wet system to an oil-wet system. This is how the wettability change is taken into account in this model.

In this model the wettability type is based on the water-oil capillary pressure values. If the water-oil capillary pressure is zero or negative there is no wettability change. Assuming that the system is initially water-wet, i.e. a positive water/oil capillary pressure, the relative permeabilities are combined with the oil-wet saturations functions as follows:

1- First the critical oil in water and water saturations are scaled:

$$S_{ocr} = FS_{ocra} + (1-F)S_{ocri} \tag{26}$$

$$S_{wcr} = FS_{wcra} + (1-F)S_{wcri} \tag{27}$$

Where S_{ocra} and S_{ocri} are the critical oil in water saturations, and S_{wcra} and S_{wcri} are the critical water saturations. The weighting factor F is a function of the volume fraction of the asphaltene deposit, which should be specified.

2- A look-up for relative permeability is then carried out on the scaled saturations from step 1, followed by a linear interpolation between the resulting water-wet and oil-wet relative permeabilities as:

$$K_{rw} = FK_{rwa} + (1-F)K_{rwi} \tag{28}$$

$$K_{row} = FK_{rowa} + (1-F)K_{rowi} \tag{29}$$

where K_{rwa} and K_{rwi} are the oil-wet and water-wet relative permeabilities to water respectively, and K_{rowa} and K_{rowi} and the oil-wet and the water-wet relative permeabilities to oil respectively.

6- Modeling the deposition of asphaltene in the slim tube

The 3-dimensional compositional simulation model of slim tube is developed and 6 experimental asphaltene deposition tests are simulated based on input data from Table 2. The initial composition of the oil is given in Table 1. The heavy component, C_{7+}, is split and characterized after fractal distribution functions. The results are given in Tables 5 and 6. It can be seen that C_{7+}, is split into 4 pseudo components: PC1, PC2, PC3 and FLOCS. The FLOCS can form asphaltene (ASPH) during the simulation.

The slim tube is initially saturated with air (based on the experiments) and different fluids at different initial pressures (injection pressures) are injected into the slim tube. Table 7 gives the composition of the injected fluids and the initial pressures of the slim tube for all tests.

Table 5. Splitting of C_{7+} after fractal distribution functions.

Component	**Oil (fraction)**
H_2S	0.0002
Nitrogen	0
CO_2	0.022
Methane	0.2694
Ethane	0.0801
Propane	0.0643
i-Butane	0.0113
n-Butane	0.0368
i-Pentane	0.0174
n-Pentane	0.0223
Hexanes	0.0420
C_{7+}	0
PC1	0.1639
PC2	0.1259
PC3	0.0332
FLOCS	0.0111
ASPH	0

Six slim tube simulation runs are performed at a temperature of 90 ^oF. The results of tests 1 to 6 are plotted in Figs. 3 and 4 respectively.

Table 6. The properties of pseudo components

omponenetC	**MW**	**Spec. Gravity**
PC1	142	0.7848
PC2	274	0.8616
PC3	351	0.8867
FLOCS	850	0.969
ASPH	850	0.969

Table 7. Composition of injection fluids and injection pressures.

	Injection fluid	**P_i (Atm)**
Test # 1	60%Oil+40%nC7	25.5
Test # 2	60%Oil+40%nC7	13.4
Test # 3	40%Oil+60%nC7	9.453
Test # 4	50%Oil+50%nC7	20.95
Test # 5	60%Oil+40%nC7	41.416
Test # 6	50%Oil+50%nC7	9.32

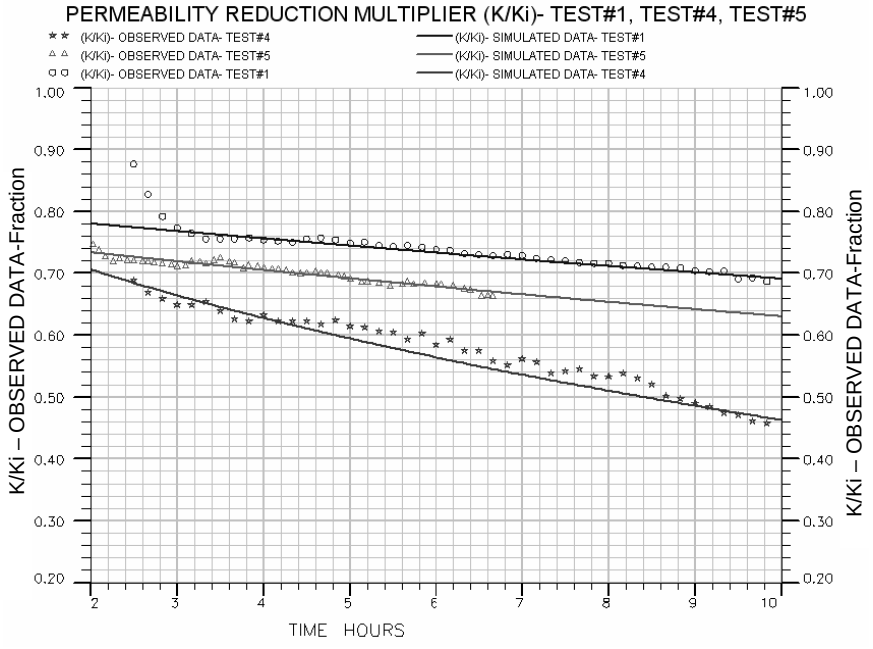

Figure 3. Comparison of simulated and experimental permeability reduction multiplier- Test#1, Test#4 and Test#5.

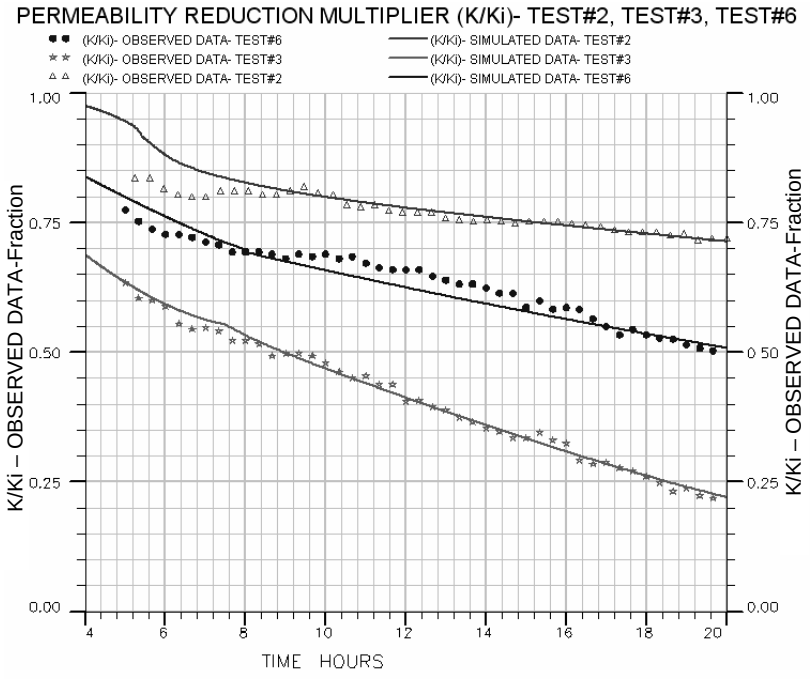

Figure 4. Comparison of simulated and experimental permeability reduction multipliers- Test#2, Test#3 and Test#6.

The following parameters are used as matching parameters:

1- Flocculation rate coefficient (r_{ia})
2- Adsorption or static deposition coefficient (α)
3- Plugging coefficient (γ)
4- Entrainment coefficient (β)
5- Exponential coefficient (δ)

As can be seen from Figs. 3 and 4, the simulated permeability reduction multipliers, due to asphaltene deposition, demonstrate good agreement with the experimental data.

7- Conclusions

The resin distribution function is the best approach for the prediction of asphaltene molecular weight distribution (MWD). We believe that this is because the base of this theoretical distribution function is the Fractal aggregation theory, which is compatible with the physics of asphaltene aggregation.

A new algorithm for static asphaltene modeling is developed. This algorithm uses a multi-solid thermodynamics approach where the fugacity for each component and phase is applied at equilibrium conditions.

Using a dynamic reservoir simulator, a 3-dimensional asphaltene model is developed to simulate the deposition of asphaltene and its impact on permeability reduction in a slim tube. The simulated permeability reduction multiplier, due to asphaltene deposition, demonstrates very good agreement with the experimental data.

References

[1] Leontaritis, K. J. "Asphaltene near-wellbore formation damage modeling". Conference paper SPE 39446, (1996).

[2] Civan, F., "Modeling and simulation of formation damage by organic deposition". Rio de Janeiro, Brazil, November 26-29, 102-107, (1995).

[3] Civan, F., Reservoir formation damage fundamentals modeling, assessment, and mitigation. Gulf Publish Company, Houston, p 742, (2000).

[4] Ali, M. A., Islam, M. R., "The effect of asphaltene precipitation on carbonate rock permeability: An experimental and numerical approach", SPE production & facilities, 178-183, (1998).

[5] Wang, S., Civan, F., "Simulation of paraffin and asphaltene deposition in porous media". SPE 50746, 57-66, (1999).

[6] Wang, S. and Civan, F. "Productivity decline of vertical and horizontal wells by asphaltene deposition in petroleum reservoirs". SPE 64991, (2001).

[7] Rassamdana, H., Sahimi, M., "Asphalt Flocculation and Deposition: II. Formation and growth of fractal aggregates". AIChE J. 42 (12), 3318–3332, (1996).

[8] Alboudwarej, H., Akbarzadeh, K., A generalized regular Solution Model for Asphaltene Precipitation from n-alkane diluted heavy oils and Bitumens. Fluid Phase Equilibria, 232, 159-170, (2005).

[9] Jorge, E.P., Monteagudo, A., Paulo, L.C., Lage, A., Rajagopal, B., Towards a poly-disperse molecular thermodynamic model for asphaltene precipitation in live-oil. Fluid Phase Equilibria, 187–188, 443–471, (2001).